THE AMERICAN SOCIETY OF MECHANICAL ENGINEERS
345 E. 47th St., New York, N.Y. 10017

95-GT-314

ENERGY ANALYSIS TO THE DESIGN OF ROTOR-BEARING SYSTEMS

W. J. Chen
Centrifugal Compressor Division
Ingersoll-Rand Company
Mayfield, Kentucky

ABSTRACT

In the design of rotating machinery, it is often desirable and necessary to change a subset of system parameters to meet the design requirements. The success in designing rotor bearing systems and/or in solving the vibration problems depends heavily upon the understanding of fundamental physical properties and insights of the systems. The modeling improvements and computational techniques have been extensively presented over the years. The design methodologies and fundamental properties have not been widely addressed to assist design engineers in solving their practical problems. The objective of this paper is to relate the various forms of energy and work and their contributions to the system dynamic characteristics. The design strategies and methodologies using the energy approach are also presented and illustrated in a turbine driven machine.

NOMENCLATURE

a,b	semi-major and semi-minor axes
$\boldsymbol{C}$	damping matrix
EI	bending modulus
F	dissipation function
$\boldsymbol{G}$	gyroscopic matrix
$\boldsymbol{g}$	intermediate matrix
I_d, I_p	diametral and polar moment of inertia
j	$\sqrt{-1}$
$\boldsymbol{K}$	stiffness matrix
$\boldsymbol{M}$	mass/inertia matrix
m_d	mass
P	axial force
$\boldsymbol{Q}$	force vector
$\boldsymbol{q}$	displacement vector
$\hat{\boldsymbol{r}}$	orbit radius vector
T	kinetic energy
t	time
$\hat{\boldsymbol{u}}$	circular motion
V	potential energy
W_{cyc}	work done per cycle
(x,y,z)	translational displacements
κGA	effective shear modulus
ϕ	phase angle
Ψ	shape functions
θ	rotational displacement
Ω	rotor speed
ω	whirl frequency

Superscripts

b,d,e,s	bearing, disk, element, support

Subscripts

c,s	cosine and sine components
f,b	forward, backward
$gyro$	gyroscopic
T,R	translation, rotation

INTRODUCTION

Over the last 20 years, there has been considerable research activity in the area of modeling and analysis of dynamic behavior of rotor-bearing-foundation systems. The dynamic characteristics of interest are critical speeds, system stability, and response to unbalance excitation. These dynamic characteristics are influenced by all the system parameters and some parameters may be more sensitive to certain dynamic behavior than others. In the design and retrofit process, it is frequently desirable and often necessary to adjust some system parameters in order to obtain a more favorable design or to meet the new operating

Presented at the International Gas Turbine and Aeroengine Congress & Exposition
Houston, Texas - June 5-8, 1995
This paper has been accepted for publication in the Transactions of the ASME
Discussion of it will be accepted at ASME Headquarters until September 30, 1995

requirements. In general, this procedure is carried out by experienced engineers with analytical tools (i.e. computer hardware and software) in an iterative process based on their experience and technical expertise. Taking advantage of rapid developments in the finite element methods and numerical optimization techniques, the design parameter changes now can be approached by systematic and automated procedures. The finite element method has been widely used in modeling and analyzing the complex rotor bearing systems with minimal numerical problems. Recently, automated optimization techniques combined with the finite element formulation in the application of rotor bearing systems have been presented by Chen (1987) to achieve the various design goals. However, caution should always be exercised while using the "black box" as a design tool. Due to the complexity of the problems, the converged solution may not always be the global optimum. The success in designing rotor bearing systems and/or in solving the vibration problems depends heavily upon the understanding of fundamental physical properties and insights of the systems.

Comprehensive coverage in computational techniques and modeling improvements has been presented in the analysis of rotor bearing systems over the years. The design strategies and methodologies have not been well addressed to assist design engineers in solving their practical problems. The use of vibration energies in the design of rotor systems was first proposed by Simmons (1976) and the emphasis was mainly on the torsional natural frequencies using the Rayleigh quotient. The design philosophy of using energy distribution in lateral vibration was presented by Gunter and Gaston (1987) in the analysis of undamped critical speeds and was briefly discussed by Nelson and Crandall (1992). The physical insights into the rotor stability using the energy (work) calculation was presented by Adams and Padovan (1981) and then was utilized by Longxiang et al. (1993) in redesigning the bearings for a 200 MV turbine generator.

The dynamic behavior of an entire rotor-bearing-foundation system is described by the governing equations of motion which are derived by the energy expressions. Therefore, the system dynamic characteristics are strongly influenced by the energy distribution. By knowing the energy distribution, one can predict the effects of parameter changes on the system behavior and identify the source of the vibration problem. This paper describes the various forms of energy and work and their contributions to the dynamics of the system. The design methodologies using energy and work are also presented. Using the energy approach, the definition of rigid and flexible rotors can be quantitatively identified. The computation of energy distribution can be easily incorporated into any existing rotor dynamics programs based on the finite element method. A 1500 KW turbine driven pump is presented to illustrate the design methodology using the energy approach.

ROTOR MOTIONS

For small vibration, the motion of a discretized finite element station is usually described by two translational displacements (x,y) in the X and Y directions respectively and two rotational (angular) displacements (θ_x, θ_y) about the X and Y axes respectively. The Z axis is the coordinate along the shaft centerline. The (X,Y,Z) axes describe a fixed global right-hand-ruled Cartesian coordinate system. In the rigorous definition, the rotational displacements depend upon the translational displacements and they can not be treated as generalized coordinates in the Lagrange's equations. However, for small displacements, they lead to linearized equations of motion. For large displacements, the Eulerian angles are normally used which lead to nonlinear equations of motion for the spinning disk. The disadvantage of using Eulerian angles is that they can not be directly expressed in the shaft element strain energy formulation without making an assumption of small displacements.

The rotor motion of most common interest is a harmonic motion with a whirl frequency of ω. At each finite element station, the rotor motion has the form:

$$x(t) = x_c \cos\omega t + x_s \sin\omega t \tag{1}$$

$$y(t) = y_c \cos\omega t + y_s \sin\omega t \tag{2}$$

for translational displacements, and

$$\theta_x(t) = \theta_{xc} \cos\omega t + \theta_{xs} \sin\omega t \tag{3}$$

$$\theta_y(t) = \theta_{yc} \cos\omega t + \theta_{ys} \sin\omega t \tag{4}$$

for rotational displacements.

This simple expression can represent a steady state synchronous unbalance response with whirl frequency ω equal to the rotor speed Ω or can be a precessional mode orbit with whirl frequency ω equal to the associated natural frequency of that mode. The whirl frequency is always a positive value, and the direction of whirling (forward or backward precession) is determined by the sign of $(x_c y_s - x_s y_c)$.

Each pair of displacements (x, y) or (θ_x, θ_y) describes an elliptical orbit with semi-major axis a and semi-minor axis b. Considering the translational orbit, the axes are:

$$a = \left\{\frac{1}{2}\left(x_c^2 + x_s^2 + y_c^2 + y_s^2\right) + \frac{1}{2}\left[\left(x_c^2 - x_s^2 + y_c^2 - y_s^2\right)^2 + 4\left(x_c x_s + y_c y_s\right)^2\right]^{1/2}\right\}^{1/2} \tag{5}$$

$$b = \frac{1}{a}\begin{vmatrix} x_c & x_s \\ y_c & y_s \end{vmatrix} = \frac{1}{a}\left(x_c y_s - x_s y_c\right) \tag{6}$$

Mathematically, a positive semi-minor axis indicates that the whirling orbit is a forward precession (progression) orbit and a negative semi-minor axis implies the motion is a backward precession (regression) orbit. In general, the rotor whirls either forward or backward. However, the rotor can also have mixed precession, i.e., the rotor can possess forward precession and backward precession simultaneously at different sections. Hence, the semi-minor axis should be evaluated at all the finite element stations to determine the direction of precession.

The elliptical orbit may also be decomposed into two circular orbits: one is a forward circular motion with a amplitude of

$|\hat{u}_f|$, and the other is a backward circular motion with a amplitude of $|\hat{u}_b|$. Thus, the displacement radius vector can be expressed in the complex form:

$$\hat{r}(t) = x(t) + j\,y(t) = |\hat{u}_f|\, e^{j\phi_f} \cdot e^{j\omega t} + |\hat{u}_b|\, e^{j\phi_b} \cdot e^{-j\omega t} \quad (7)$$

When the forward amplitude is greater than the backward amplitude, the overall rotor motion is forward. When the backward amplitude is greater than the forward amplitude, the resulting motion is backward. The relationship between the semi-axes and the amplitudes of the circular motions are:

$$a = |\hat{u}_f| + |\hat{u}_b|, \quad \text{and} \quad b = |\hat{u}_f| - |\hat{u}_b| \quad (8)$$

The above expressions are also applicable to the rotational displacements.

The motions of non-rotating components (flexible support, foundation) can be described by a total of six degrees of freedom including axial translation and rotation, although four degrees of freedom are commonly utilized.

EQUATIONS OF MOTION AND ENERGY

The equations of motion which describe the dynamic behavior of the entire rotor system are obtained by assembling the equations of motion of the appropriate components. The governing equations of motion for a general rotor-bearing-foundation system is of the form:

$$\boldsymbol{M}\ddot{\boldsymbol{q}}(t) + (\boldsymbol{G} + \boldsymbol{C}^b)\dot{\boldsymbol{q}}(t) + (\boldsymbol{K} + \boldsymbol{K}^b)\boldsymbol{q}(t) = \boldsymbol{Q}(t) \quad (9)$$

where $\boldsymbol{q}$ and $\boldsymbol{Q}$ are the system displacement and force vectors respectively. The mass/inertia matrix $\boldsymbol{M}$ is a positive definite real symmetric matrix which is contributed by the kinetic energy. The gyroscopic matrix $\boldsymbol{G}$ is a real skew-symmetric matrix which is contributed by the part of the rotational kinetic energy caused by the gyroscopic moments. The structural stiffness matrix $\boldsymbol{K}$ is a real symmetric matrix contributed by the strain energy. The bearing coefficient matrices $\boldsymbol{C}^b$ and $\boldsymbol{K}^b$, in general, can be any real non-symmetric matrices due to the fact that bearings are non-conservative in nature. Since the equations of motion are derived from the energy expressions, the system dynamic characteristics are strongly influenced by the energy distribution. A typical rotor system consists of discrete rigid disks, shaft elements with distributed mass and elasticity, general linear bearings, and flexible bearing supports. The various forms of energy for these components are presented below.

Rigid Disks

The kinetic energy of a spinning disk with translational and rotational motion may be expressed in a fixed coordinate system as the sum of the translational and rotational kinetic energies (Dimentberg, 1961):

$$\begin{aligned} T^d &= \frac{1}{2} m_d (\dot{x}^2 + \dot{y}^2) + \frac{1}{2} I_d (\dot{\theta}_x^2 + \dot{\theta}_y^2) \\ &\quad + \frac{1}{2}\Omega I_P (\dot{\theta}_x \theta_y - \theta_x \dot{\theta}_y) + \frac{1}{2}\Omega^2 I_P \end{aligned} \quad (10)$$

The first two terms are homogeneous quadratic functions of the generalized velocities and are commonly presented in a natural system (Meirovitch, 1980). The first term is the translational kinetic energy contributed by the disk mass effect. The second term is a fraction of the rotational kinetic energy contributed by the rotatory inertia. The first two terms are always positive. The third term is linear in the generalized velocities and is referred to as the gyroscopic effect which is contributed by the gyroscopic moments. The fourth term, caused by the pure spinning of the disk, does not depend upon the vibration coordinates and can be ignored in the vibrational analysis. Due to the gyroscopic effect, the kinetic energy given in equation (10) is known as nonnatural (Meirovitch, 1980) and the effect also makes the rotordynamics study unique from the general structural dynamics.

To gain insight into the gyroscopic effect, substituting the rotational displacements in equations (3) and (4) and their derivatives into the rotational kinetic energy generated by the gyroscopic effect, we have

$$\begin{aligned} T_{gyro} &= \frac{1}{2}\Omega I_P (\dot{\theta}_x \theta_y - \theta_x \dot{\theta}_y) = \frac{1}{2}\Omega I_P \omega\, (\theta_{xs}\theta_{yc} - \theta_{xc}\theta_{ys}) \\ &= \frac{1}{2}\Omega I_P \omega \left(-a \cdot b\right) = \frac{1}{2}\Omega I_P \omega \left(-|\hat{u}_f|^2 + |\hat{u}_b|^2\right) \end{aligned} \quad (11)$$

where a, b, and $|\hat{u}_f|$, $|\hat{u}_b|$ in equation (11) are parameters for the rotational displacement orbit. Since I_P, Ω, ω are all positive values, the sign of equation (11) is determined by the value inside the parenthesis. For the forward precessional mode ($b > 0$), the gyroscopic effect contributes negative kinetic energy (much like inertia decreased effect) and tends to raise the corresponding forward whirl frequency. For the backward precessional mode ($b < 0$), the gyroscopic effect contributes positive kinetic energy (much like inertia added effect) and tends to lower the corresponding backward whirl frequency. Thus, it is the forward vibrational modes getting the "gyroscopic stiffening" effect and the backward vibrational modes getting the "gyroscopic softening" effect. The gyroscopic effect is linearly proportional to the polar moment of inertia, spinning speed, whirl frequency, and area of rotational displacement whirl orbit. It can be significant in the study of high speed overhung rotor system where a large wheel is mounted outside the bearing span and has large rotational displacement.

The coefficient matrices in the equations of motion can be obtained from the Lagrange's equations or can be easily identified by expanding the energy expression in matrix form. The kinetic energy of a spinning disk excluding the spinning effect, $\frac{1}{2}\Omega^2 I_P$, can be conveniently written in matrix form:

$$T^d = \frac{1}{2}\dot{\boldsymbol{q}}^{dT}(\boldsymbol{M}_T^d + \boldsymbol{M}_R^d)\dot{\boldsymbol{q}}^d + \boldsymbol{q}^{dT}(\boldsymbol{g}^d)\dot{\boldsymbol{q}}^d \quad (12)$$

where $\boldsymbol{q}^d(t) = (x, y, \theta_x, \theta_y)^T$ is the displacement vector of the finite element station at which the disk is located. The symmetric matrices $\boldsymbol{M}_T^d$ and $\boldsymbol{M}_R^d$ are the translational mass matrix and rotational inertia matrices, respectively. The only non-zero elements in these matrices are the (1,1) and (2,2) elements with a value of m_d and I_d in $\boldsymbol{M}_T^d$ and $\boldsymbol{M}_R^d$ respectively. The gyroscopic matrix $\boldsymbol{G}^d$ is a skew-symmetric matrix derived from the intermediate skew-symmetric matrix $\boldsymbol{g}^d$:

$$\boldsymbol{G}^d = \left(\boldsymbol{g}^d\right)^T - \boldsymbol{g}^d = -2\boldsymbol{g}^d = \Omega I_P \begin{bmatrix} 0 & 0 & 0 & 0 \\ 0 & 0 & 0 & 0 \\ 0 & 0 & 0 & 1 \\ 0 & 0 & -1 & 0 \end{bmatrix} \quad (13)$$

The rigid disks possess only kinetic energy, not potential energy.

Shaft Elements

The kinetic energy of a finite element segment is obtained by integrating the differential energy for an infinitesimal rotor element over the length of the element:

$$T^e = \frac{1}{2}\left\{\int_0^l \tilde{m}(\dot{x}^2 + \dot{y}^2) + \tilde{I}_d(\dot{\theta}_x^2 + \dot{\theta}_y^2) + \Omega\tilde{I}_p(\dot{\theta}_x\theta_y - \theta_x\dot{\theta}_y)\, ds\right\}$$
$$+\frac{1}{2}\Omega^2\int_0^l \tilde{I}_p\, ds \quad (14)$$

Since the internal displacements $(x, y, \theta_x, \theta_y)$ are functions of spatial coordinate (s) and time (t), the finite element method is utilized to separate the variables. The internal displacements of a typical element can be approximately expressed by the following relationship:

$$\begin{Bmatrix} x(s,t) \\ y(s,t) \\ \theta_x(s,t) \\ \theta_y(s,t) \end{Bmatrix}_{4x1} = \begin{bmatrix} \Psi_T(s) \\ \Psi_R(s) \end{bmatrix}_{4x8} \boldsymbol{q}^e(t)_{8x1} \quad (15)$$

The displacement vector $\boldsymbol{q}^e(t) = (q_1, q_2, q_3, \ldots, q_7, q_8)^T$ is the time dependent end-point displacements (two translations and two rotations) of the finite rotor element. The shape function matrix, Ψ, is established by utilizing the Timoshenko Beam Theory which includes the transverse shear deformation effect. The individual shape functions represent the static displacement modes associated with a uniform Timoshenko beam with a unit displacement of one of the end-point coordinates and the rest of the coordinates constrained to zero. The derivation of the shape function is well documented (Nelson, 1977) and will not be repeated here.

Substituting equation (15) into the element kinetic energy expression and neglecting the last term (spinning energy), which does not depend upon the displacements, we have:

$$T^e = \frac{1}{2}\dot{\boldsymbol{q}}^{eT}(\boldsymbol{M}_T^e + \boldsymbol{M}_R^e)\dot{\boldsymbol{q}}^e + \boldsymbol{q}^{eT}(\boldsymbol{g}^e)\dot{\boldsymbol{q}}^e \quad (16)$$

where

$$\boldsymbol{M}_T^e = \int_0^l \tilde{m}\,\Psi_T^T\Psi_T\, ds$$

is the translational mass matrix,

$$\boldsymbol{M}_R^e = \int_0^l \tilde{I}_d\,\Psi_R^T\Psi_R\, ds$$

is the rotational inertia matrix, and

$$\boldsymbol{g}^e = \int_0^l \frac{1}{2}\Omega\tilde{I}_p\,\Psi_R^T\begin{bmatrix} 0 & -1 \\ 1 & 0 \end{bmatrix}\Psi_R\, ds$$

is the intermediate skew-symmetric matrix. The element gyroscopic matrix is:

$$\boldsymbol{G}^e = \left(\boldsymbol{g}^e\right)^T - \boldsymbol{g}^e = -2\boldsymbol{g}^e = \int_0^l \Omega\,\tilde{I}_p\Psi_R^T\begin{bmatrix} 0 & 1 \\ -1 & 0 \end{bmatrix}\Psi_R\, ds \quad (17)$$

The potential (strain) energy of the rotating shaft element consists of elastic bending energy due to the bending moments, shear energy due to the shear forces, and work due to the constant axial load. The translational displacements of a typical point internal to the element consists of the deformations due to bending moment and shear force. However, the rotational displacements are only related to the bending deformation. An element under shear force alone will only possess distorsion but no rotation. The potential energy of a rotating shaft element under a constant axial load is:

$$V^e = \frac{1}{2}\int_0^l EI\left[\left(\frac{\partial\theta_x}{\partial z}\right)^2 + \left(\frac{\partial\theta_y}{\partial z}\right)^2\right]ds +$$
$$\frac{1}{2}\int_0^l \kappa GA\left[\left(\frac{\partial x}{\partial z} - \theta_y\right)^2 + \left(\frac{\partial y}{\partial z} + \theta_x\right)^2\right]ds + \quad (18)$$
$$\frac{1}{2}\int_0^1 P\left[\left(\frac{\partial x}{\partial z}\right)^2 + \left(\frac{\partial y}{\partial z}\right)^2\right]ds$$

where EI is the bending modulus, κGA is the effective shear modulus, and P is the axial load. The shape factor κ depends on the shape of the cross section and Poisson's ratio. Substituting the shape functions relationship, the potential energy can be conveniently written in matrix form:

$$V^e = \frac{1}{2}\boldsymbol{q}^{eT}\left[\boldsymbol{K}_b + \boldsymbol{K}_s + \boldsymbol{K}_a\right]\boldsymbol{q}^e \quad (19)$$

where

$$\boldsymbol{K}_b = \int_0^l EI\left(\Psi_R''\right)^T\left(\Psi_R''\right)ds$$

is the bending stiffness matrix,

$$\boldsymbol{K}_s = \int_0^l \kappa GA\left(\Psi_T'' + \begin{bmatrix} 0 & -1 \\ 1 & 0 \end{bmatrix}\Psi_R\right)^T\left(\Psi_T'' + \begin{bmatrix} 0 & -1 \\ 1 & 0 \end{bmatrix}\Psi_R\right)ds$$

is the shear stiffness matrix, and

$$\boldsymbol{K}_a = \int_0^l P\left(\Psi_T'\right)^T \left(\Psi_T'\right) ds$$

is the geometric stiffness matrix due to axial load.

The above shaft element stiffness matrices are all symmetric. The shear deformation effect can be important when analyzing a short stubby rotor system. Since the effect of shear deformation is included in the "shape functions" of the elements, therefore, it is taken into account not only in the potential energy calculation but also in the kinetic energy calculation. The total effect of the shear deformation is to lower the natural frequencies. The geometric stiffness matrix is positive when the element is under tensile load and negative when the element is under compressive force.

Flexible Supports

For the flexible bearing support, the kinetic energy and potential energy are of the forms:

$$T^s = \frac{1}{2}\dot{\boldsymbol{q}}^{sT}\boldsymbol{M}^s\dot{\boldsymbol{q}}^s \tag{20}$$

and

$$V^s = \frac{1}{2}\boldsymbol{q}^{sT}\boldsymbol{K}^s\boldsymbol{q}^s \tag{21}$$

where $\boldsymbol{q}^s$ is the displacement vector of the support and the mass and stiffness matrices are symmetric.

Linear Bearings

The linear bearings are generally modeled by eight bearing dynamic damping and stiffness coefficients. The associated dissipation function and potential energy are assumed to be derived from the following quadratic expressions:

$$F^b = \frac{1}{2}\dot{\boldsymbol{q}}^{bT}\boldsymbol{C}^b\dot{\boldsymbol{q}}^b \tag{22}$$

and

$$V^b = \frac{1}{2}\boldsymbol{q}^{bT}\boldsymbol{K}^b\boldsymbol{q}^b \tag{23}$$

where $\boldsymbol{q}^b$ is the displacement vector associated with the bearing coordinates. For fluid film bearings, the forces are non-conservative and the damping and stiffness matrices are non-symmetric. The damping provides stabilizing forces to attenuate the resonant response and to overcome the disturbance. However, the cross-coupling stiffness can introduce a major destabilizing effect on the rotor system. The work done on the system (negative energy removed from the system) by a bearing per cycle of a harmonic motion is:

$$\begin{aligned} W_{cyc} = -\pi\omega[&C_{xx}(x_c^2 + x_s^2) + C_{yy}(y_c^2 + y_s^2) + \\ &(C_{xy} + C_{yx})(x_c y_c + x_s y_s)] \\ +\pi&(K_{xy} - K_{yx})\,(a \cdot b) \end{aligned} \tag{24}$$

With the positive $(K_{xy} - K_{yx})$, the cross-coupling stiffness can actually add energy to the system for a forward precessional motion ($b > 0$) and destabilize the rotor system in the linear sense. Another interesting finding is that the cross-coupling damping coefficients can also either remove energy from the system or add energy to the system. This work done by the bearing can provide rich information in the determination of bearing sensitivity to the system stability.

Seal forces, aerodynamic forces, and other interaction forces acting on the rotors can be modeled as pseudo bearings.

DESIGN METHODOLOGY

The objectives in the design of rotor systems include the placement of critical speeds, minimization of unbalance response, and maximization of the system stability. Since the system dynamic behavior is governed by the equations of motion and the system matrices are constructed by the various energies, the system dynamic characteristics depend upon the energy distribution. The analytical calculation of critical speeds, damped eigenvalues, and forced response from the equations of motion, eq. (9), is documented in Nelson and Crandall (1992) and will not be repeated here. However, the general design methodology and criteria using energies are described below. It should be noted that the energy is also closely related to the mode shape and the amplitude of a vibration mode is a normalized eigenvector, thus the energy distribution is calculated as a percentage of the total energy of that particular mode.

Critical Speeds

The most primary consideration in the design of rotating machinery is the placement of forward synchronous critical speeds with respect to the operating speed of the machine. The other dynamic behavior (e.g. unbalance response and system stability) are all somewhat related to the position of the critical speeds. When the critical speeds are within the operating speed range, the rotor may experience large synchronous vibration. When the first critical speed is too low (e.g. lower than or around 50% of the design speed), the rotor may be susceptible to instability and experience high sub-synchronous vibration. When the rotor is operated far below the first critical speed, it can be sensitive to the operating environment. Since damping has little effect on the position of the critical speeds, the undamped system has been widely used to predict critical speeds. Damping effects are considered in the unbalance response and system stability analyses.

Whenever possible, it is desirable to have at least 15% (10% is required in most standards) separation margin between the operating speed and the critical speeds to ensure safe and smooth operation. When the critical speeds are within the undesirable range, some parameters need to be adjusted to shift the critical speeds outside this operating range. Bearing stiffnesses, mass properties of the disks, and shaft elements of the rotating assemblies are usually the variables that can be changed to achieve this requirement. Bearing locations have a great influence in positioning the critical speeds, however, they can not be easily changed in an existing design without major modification in the layout and general arrangement.

If the bearing stiffnesses are the only variables that can be changed, then one should look to those bearings with high

potential energy density. If a particular bearing has very small potential energy density (e.g. less than 5%) of a particular mode, then minor modification in this bearing has little effect on that mode. In fact, increasing the bearing stiffness will have an adverse effect due to the reduction in the modal damping. An increase or decrease in diameter of the shaft elements with large potential energy density can be used to effectively raise or lower the critical speed. Decreasing or increasing the mass of a disk with high translational kinetic energy density can also significantly increase or decrease the critical speed. Caution must be taken to ensure that the center of gravity of the disk will not be moved while changing the mass properties of the disk. Also, decreasing or increasing the polar moment of inertia of a disk, which has high rotational kinetic energy density, can decrease or increase the critical speed due to the gyroscopic effects. If the kinetic and potential energies of a vibration mode are significant in the flexible bearing supports, changing the support structure can be very effective in shifting that associated frequency. For the support modes, the non-contact displacement probes measuring the shaft vibration may not be enough for a safe monitoring system and an accelerometer or velocity pickup on the bearing housing may be required.

The potential energy distribution among the rotor assembly, bearings, and flexible supports can also provide information for design purposes. If the rotor assembly (shaft elements) possesses more than 70% of the total potential energy of a vibration mode, then this vibration mode is characterized as a flexible rotor mode. If the rotor assembly (shaft elements) possesses less than 30% of the total potential energy of a vibration mode, then this vibration mode is characterized as a rigid rotor mode. Typically, the first two lowest frequency modes are the rigid rotor modes and other high frequency modes are flexible rotor modes. In some cases, the rigid rotor modes could be overdamped or could not be excited by the synchronous excitation, thus they will not be observed in the response data. For rotors operated above the rigid bearing criticals (e.g. most high speed compressors), it is desirable to design the bearings such that the potential energy of the critical speed can be evenly distributed among the rotor and bearings. If the critical speed falls into the rigid rotor section, the system will be more susceptible to instability (e.g. oil whirl or whip) and the vibration could be large enough in the bearing station to damage the bearing. If the critical speed falls into the flexible rotor section, the vibrations may be very large at some critical stations due to the lack of damping.

The damped critical speeds are usually determined from the whirl speed map which is a plot of damped natural frequencies (whirl speeds) versus the rotor speed. The damped critical speeds due to the synchronous unbalance excitation are the intersections of the synchronous excitation line and the frequency curves. In the presence of gyroscopic effect and the general linearized bearing model, the frequency curves may be overlapping and complicated. The associated precessional mode shapes must be used to identify the modes and properly construct the map.

Unbalance Response and Balancing

The rotors always have some amount of residual unbalance no matter how well they are balanced. Very often some correction weights are needed to minimize the response at certain locations. Unbalance located at large modal displacements will produce a large modal unbalance force for that mode. Usually, the unbalance weights may only be placed or removed at certain disks. Therefore, one should look to the disks with large kinetic energy density to make corrections. A caution must be made since corrections for one particular mode may be quite different from that of another mode. The influence coefficient method combined with energy distribution information can be very effective in balancing which may eliminate unnecessary trial runs.

System Stability

The system stability is usually determined by the value of logarithmic decrement. The instability threshold is determined from the stability map which is a plot of logarithmic decrements versus the rotor speed. When the logarithmic decrement is positive, the system is said to be stable. When the logarithmic decrement becomes negative, the system is said to be unstable in the linear theory. When the logarithmic decrement is zero, the system is in the state of instability threshold. Assuming that only the bearings (real or pseudo) remove/add energy from/to the system, the total energy removed/added by the bearings can also be used to determine the system stability. When the total work done on the system by the bearings is negative (i.e. energy has been removed by the bearings), the system is stable. When the total work done on the system by the bearings is positive, the system is unstable. At the threshold of instability, the total work done equals zero. By knowing the work distribution, one can not only determine the system stability but also determine the sensitivity and contribution of each bearing to the system stability. The latter information is extremely useful to the engineers in the design and retrofit process and this information does not exist by knowing the logarithmic decrement alone.

The system stability is strongly influenced by the bearings with large work done. The bearings with negative work contribute stabilizing effects and the bearings with positive work contribute destabilizing effects. If required, one should always try to maximize the energy removed by the bearings to increase the system stability. It should be noted that the bearing contribution at different vibration modes can be quite different. One question that should always be raised before any bearing modification is "what vibration mode do we want to stabilize"? Once the question is answered, work done by the bearings on the specified vibration mode is then calculated and tabulated. Bearings with large work done should be redesigned first. In this economic and efficiency conscious age, designing bearings to maximize stability and also minimize frictional power loss can be a difficult task.

EXAMPLE

A turbine driven pump is employed as an example. The complete rotor assembly is supported by three 2-axial groove bearings as shown in Figure 1. On the left side of bearing #2 is a turbine and on the right side is a pump. The design speed is

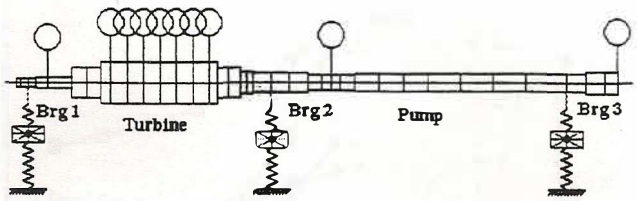

FIG. 1 SYSTEM CONFIGURATION

3500 rpm. However, the actual operating speed can fluctuate from 3000 to 4000 rpm under various operating conditions.

The whirl speed map is plotted in Figure 2. The first seven damped natural frequencies, which are below 5000 rpm, are plotted. The modes are numbered according to the values of their associated frequencies at a rotor speed of 3500 rpm. The logarithmic decrements of these modes are plotted in Figure 3. The logarithmic decrement of the fourth mode is very high (above 10), therefore, it is not shown in Figure 3. The first mode is a forward mode with most of the motion occurring at the turbine, as shown in Figure 4. Shaft elements around bearing #1 possess most of the shaft potential energy and bearing #2 possesses most of the bearing potential energy. This mode becomes unstable when the rotor speed is above 3675 rpm as shown in Figure 3. The second mode is a forward mode with most of the motion occurring at the pump side. The first two modes are excited by the synchronous excitation around 1500 and 1600 rpm. Since the logarithmic decrements at these critical speeds are relatively high (above 0.5), smooth operation through these critical speeds is anticipated. The third and fifth modes are also forward modes. These two modes are excited by the synchronous excitation around 2400 rpm and some vibration is anticipated due to the relatively low logarithmic decrement (below 0.25) in the third mode. The third and fifth critical speed modes have very similar mode shapes with one associated with the X-Z plane and the other associated with the Y-Z plane. The undamped planar mode shape is plotted in Figure 5. The total kinetic energy is distributed between the disks (64 percent) and shaft elements (36 percent). The supports have less than one percent of the total kinetic energy. The total potential energy is distributed between the bearings (32 percent) and shaft elements (68 percent). Again, the supports have an insignificant effect in the potential energy. Clearly, the mode is not sensitive to the supports. The shaft energy distributions are plotted in Figure 6 with the kinetic energy in the upper half and potential energy in the lower half. Figure 6 shows that the shaft elements of the pump are more sensitive to this mode than those of the turbine since the pump possesses most of the kinetic and potential energies. The energy distributions for disks and bearings are plotted in Figure 7. It shows that bearings #2 and #3 have a strong influence on this critical speed and that bearing #1 has almost no influence on this mode. Figure 7 also shows that disk #10 (impeller of the pump) has a significant effect on this mode due to its 55 percent contribution to the total kinetic energy. Changing the mass properties of disk #10 can be very effective in shifting this critical speed. The fourth mode is a bearing mode. All the motion occurs near bearing #1 and the logarithmic decrement is very high (above 10). The sixth mode is a backward precessional mode which is not likely to be excited by the unbalance. There is a safe separation margin between the critical speeds and the operating speed in this application.

The instability (negative logarithmic decrement) occurring around 3675 rpm poses a possible problem since the rotor speed can go up to 4000 rpm. To understand the bearing contribution to the system stability, the work done by the bearings to the unstable mode is plotted in Figure 8. It shows that the total work done is negative when the rotor speed is below 3675 rpm and becomes positive when the rotor speed is above this instability threshold. Figure 8 also shows that bearing #2 has a significant contribution to the instability and bearing #3 has little influence on the instability. To correct the instability problem, a 5-pad tilting pad bearing is recommended to replace the 2-axial groove bearing in bearing #2. The onset of instability threshold with this modification is raised to 4375 rpm which is outside the operating speed range. Again, the work done by the bearings is plotted in Figure 9. The total work done by the bearings is negative when the rotor speed is below 4375 rpm and becomes positive when the rotor speed is above 4375 rpm.

CONCLUSION

The calculation methods on various forms of energy and work have been presented. The energy computation can be easily incorporated into any existing rotor dynamics programs based on the finite element method. The contribution of energy and work to the dynamics of rotor systems has been described. The dynamic characteristics of rotor-bearing-foundation systems are strongly influenced by the energy distribution. Knowing the energy distribution, one can predict the effects of parameter changes on the system behavior and identify the source of the vibration problem. The design methodologies using energy and work have been presented. A 1500 KW turbine driven pump has been analyzed to illustrate the design methodology.

APPENDIX

The shape factor κ for a hollow circular cross-section beam is given by:

$$\kappa = \frac{6\,(1+\nu)\,\left(1+\Re^2\right)^2}{(7+6\nu)\,\left(1+\Re^2\right)^2 + (20+12\nu)\Re^2} \qquad \text{(A1)}$$

where ν is the Poisons' ratio and $\Re = r_i / r_o$ is the ratio of inner to outer diameter. The most common cases used in the rotor dynamics analysis are:

For a solid shaft, $\kappa = \dfrac{6(1+\nu)}{(7+6\nu)}$ (for ν=0.3, κ=0.886)

For a thin-walled tube, $\kappa = \dfrac{2(1+\nu)}{4+3\nu}$ (for ν=0.3, κ=0.531)

REFERENCES

Adams, M. L. and Padovan, J., 1981, "Insights Into Linearized Rotor Dynamics," *Journal of Sound and Vibration*, Vol. 76, pp. 129-142.

Chen, W. J., 1987, "Optimal Design and Parameter Identification of Flexible Rotor-Bearing Systems," Ph.D. Dissertation, Arizona State University, Tempe, Arizona.

Dimentberg, F. M., 1961, *Flexural Vibrations of Rotating Shafts*, Butterworth, London.

Gunter, E. J. and Gaston, C. G., 1987, "CRITSPD-PC User's Manual: A program for Undamped Critical Speed Analysis of Flexible Rotor-Bearing Systems," RODYN Vibration, Inc., Charlottesville, VA.

Longxiang, X., Jun. Z., and Lie, Y., 1993, "Contribution Factor of Bearings for Rotor-Bearing System stability," *ASME Journal of Vibration and Acoustics*, Vol. 115, pp.81-84.

Meirovitch, L., 1980, Computational Methods in Structural Dynamics, Sijthoff & Noordhoff International Publishers B. V., Alphen aan den Rijn, The Netherlands.

Nelson, H. D., 1977, "A Finite Rotating Shaft Element Using Timoshenko Beam Theory," Report ERC-R-77023, Arizona State University, Tempe, Arizona.

Nelson, H. D. and Crandall, S. H., 1992, "Chapter 2 - Analytic Prediction of Rotordynamic Response", *Handbook of Rotordynamics*, Edited by F. F. Ehrich, Mcgraw-Hill, Inc..

Simmons, H. R., 1976, "Vibration Energy:A Quick Approach to Rotor Dynamic Optimization," *ASME* Paper 76-Pet-60.

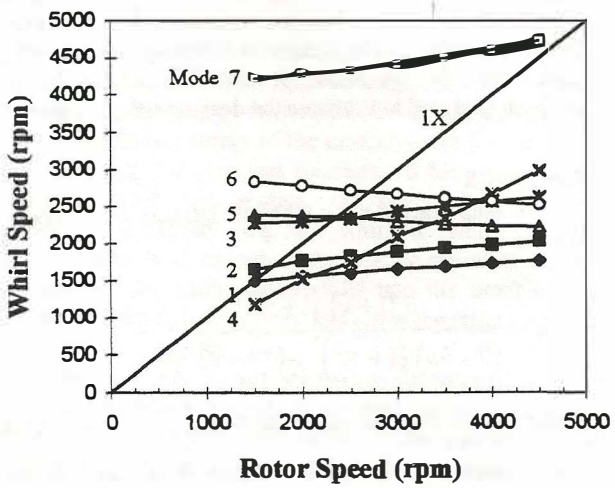

FIG. 2 WHIRL SPEED MAP

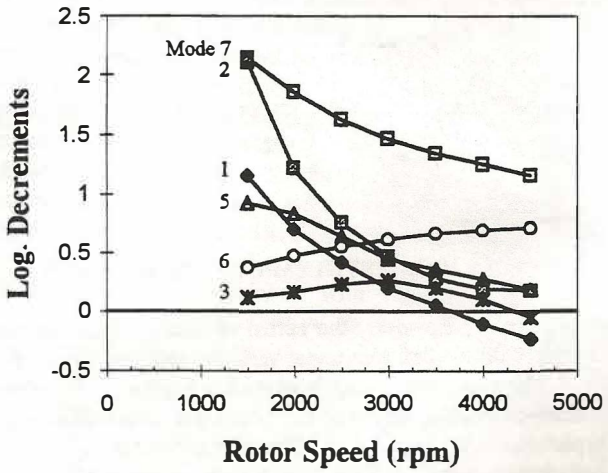

FIG. 3 STABILITY MAP

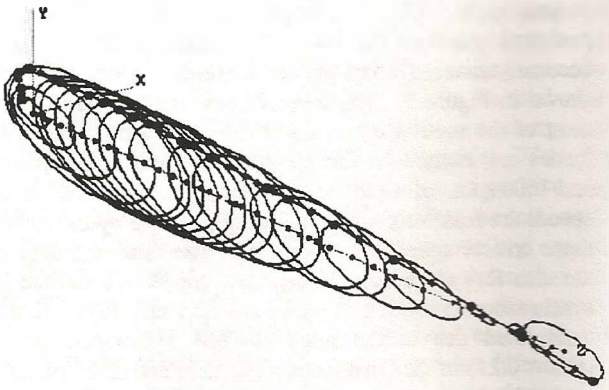

FIG. 4 FIRST FORWARD MODE SHAPE

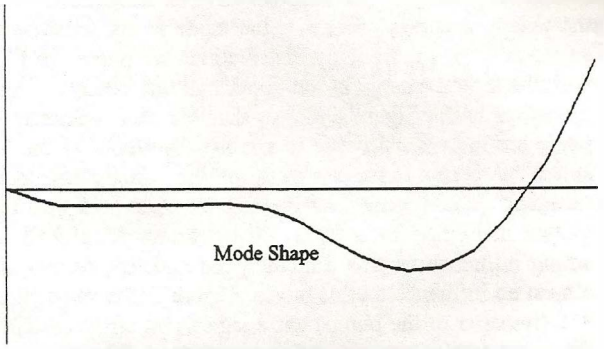

FIG. 5 THE THIRD CRITICAL SPEED

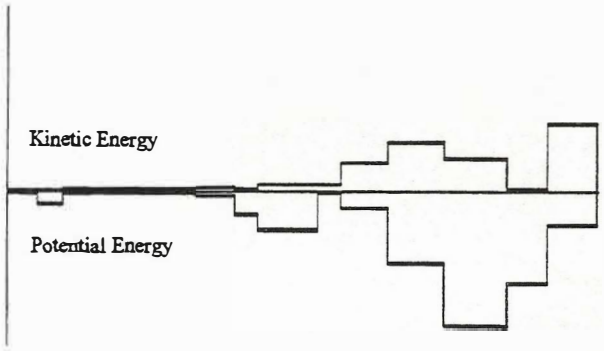

FIG. 6 SHAFT ENERGY DISTRIBUTION

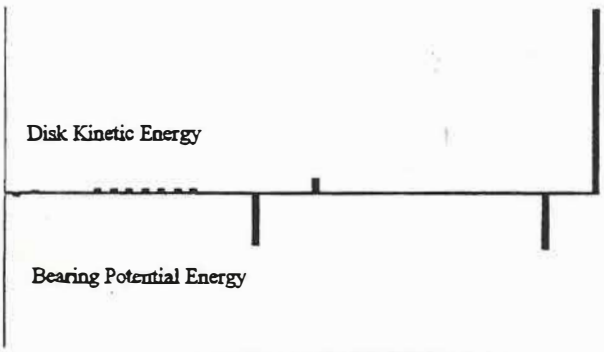

FIG. 7 BEARING AND DISK ENERGIES

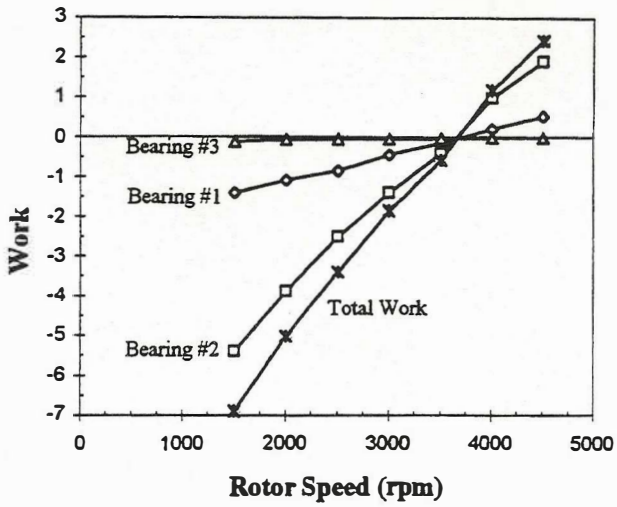

FIG. 8 BEARING WORK DISTRIBUTION

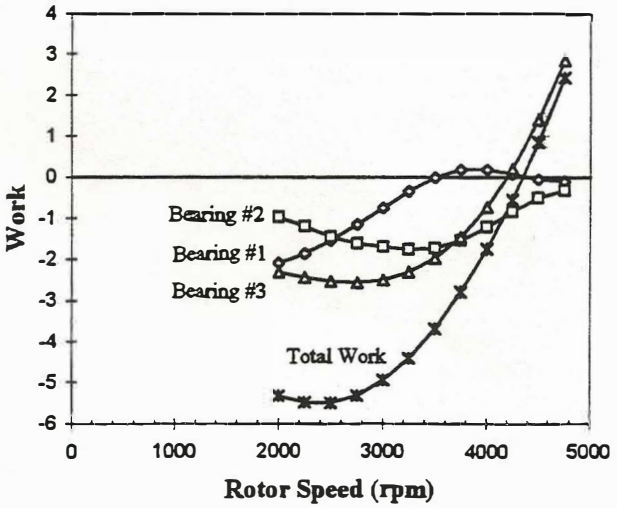

FIG. 9 BEARING WORK DISTRIBUTION (NEW DESIGN)